Meta-analysis reveals the tempo of evolutionary parallelism of local adaptation between native and introduced ranges of invasive plant species

Romane Normand[a,*], Alexis Heckley[b,c], Kathryn Hodgins[d], Samantha Grover[e], Tim Connallon[d,†], Akane Uesugi[a,†]

[a] Department of Biology, School of Science, RMIT University, Bundoora, VIC 3083, Australia

[b] Department of Biology, McGill University, Montréal, Quebec, Canada

[c] School of Biological Sciences, University of Oklahoma, Norman, OK, USA

[d] School of Biological Sciences, Monash University, Clayton, VIC 3800, Australia

[e] Applied Chemistry and Environmental Science, School of Science, RMIT University, Melbourne, VIC 3000, Australia

[*] Corresponding author

[†] Equal contributions

Abstract

Invasive species are valuable systems for evaluating evolutionary predictability, as populations in native and introduced ranges evolve separately, yet often encounter similar environmental challenges that select for parallel patterns of local adaptation. However, it remains unclear how pervasive and strong such parallelism is and how rapidly it evolves. To address these questions, we first extended cline theory to predict evolutionary patterns of parallelism between ranges. We then carried out a meta-analysis of clinal divergence in native and introduced populations of the same plant species and evaluated the tempo of evolutionary parallelism between ranges. Clines in introduced ranges were, on average, slightly shallower than native range clines for size, morpho-physiology, and phenology traits, but similar for reproductive and defense traits. Evolutionary parallelism of clinal divergence strongly increased with the time since introduction, with the greater parallelism in older introductions primarily caused by increased alignment in the direction of clinal divergence between ranges rather than changes in their relative magnitudes of divergence. These results are consistent with a two-phased process of cline evolution, in which introduced clines initially arise by drift during the range expansion, and subsequently evolve in response to local selection, ultimately leading to strong parallelism with the native range.

Keywords: clinal divergence | evolutionary convergence | evolutionary predictability | environmental gradients | invasive species

Introduction

A general understanding of the process of adaptation must address several broad questions about how ecology, evolution and genetics interact in natural populations. How predictable is evolution? Do shared environmental conditions lead to reliably parallel evolutionary outcomes [1,2], or are there multiple genetic or phenotypic solutions to the same environmental challenges [3]? Do populations typically adapt rapidly over ecological timescales [4,5], or do they experience sustained evolutionary lags in adaptation to their environments, owing to limited genetic variation or other constraints [6,7]? What are the key environmental variables—abiotic and biotic—that determine natural selection and the direction of evolutionary change [8,9]? Each of these questions is difficult to answer, especially in natural systems.

Introduced species provide exceptional study systems for addressing questions about adaptation, including its predictability, rate, and genetic basis [10,11]. For example, shared environmental factors between the native and introduced ranges of a species can favor parallel local adaptation between ranges ("parallelism"), resulting in geographically similar patterns of spatial divergence along temperature, aridity, or other spatial gradients in the environment (e.g., [12–14]). In other cases, evolutionary contingency or environmental differences between the ranges can promote evolutionary divergence between native versus introduced populations (e.g., [15,16]). In addition, the age of an introduction constrains the time available for adaptation. In some cases, rapid evolutionary diversification across the new range may keep pace with the range expansion itself, leading to substantial local adaptation within decades of the introduction [17,18]. In other cases, introduced populations may experience evolutionary lags, with protracted periods of suboptimal local adaptation across their introduced ranges [19,20]. Finally, these phenomena may play out differently among trait types [21], which may show differences in the strength or direction of selection that they experience, or in their genetic capacities for evolutionary change.

Comparisons of native and introduced populations of the same species offer two major advantages for evaluating the evolutionary rate and predictability of local adaptation. First, such studies have a natural, paired design, akin to case-control experiments, in which the evolution of a common set of traits can be directly compared across the native and introduced ranges [22]. Such comparisons are particularly powerful when carried out using individuals reared in common garden environments [21], which allow evolved differences among populations to be isolated from environmental factors. One can then directly contrast the direction and steepness of geographic clines across the introduced range, whose populations are relatively recent and potentially maladapted to their local conditions, with the native range, whose populations have had extensive time to evolve and are presumably better adapted to local conditions [23,24]. Second, introduction dates are well-documented in historical records, which provides opportunities to quantitatively test whether indices of local adaptation (*e.g.*, clines in introduced ranges and parallelism with native range clines) become stronger as the time since the introduction increases [25,26]. If selection favors similar trait–environment relationships in both ranges, older introductions should exhibit greater parallelism than more recent introductions [27].

Studies of local adaptation in native versus introduced populations of the same species have progressed to a point where we now have many high-quality case studies spanning a diverse range of plant taxa [21]. These studies, if analyzed in a common framework, provide an opportunity to test hypotheses about local adaptation, including the degree and tempo of parallelism between native and introduced portions of species' ranges. With this goal in mind, we conducted a systematic search for common-garden trait cline studies in plants and identified 34 studies, spanning 23 species and 465 traits, that report cline estimates in both the native and introduced portions of the species' range. Our dataset expands upon earlier meta-analyses of

trait clines in native versus introduced plant populations by incorporating studies published over the last 15 years ([21] includes studies published up to 2011).

We begin by presenting an extension of classical cline theory that generates quantitative predictions for the evolution of cline parallelism between native and introduced ranges of a species. We then carry out an analysis of published cline data to address three questions: (1) How predictable is local adaptation, as implied by evolutionary parallelism of trait clines between native and introduced ranges? (2) How rapid is the evolution of local adaptation, as implied by the interaction between the time since introduction and the degree of parallelism between introduced and native populations? (3) To what extent do different trait categories (e.g., morphological, phenological, and defense traits) vary in their degree of parallelism or in their evolutionary lags in introduced ranges?

Trait clines in native versus introduced ranges: Theoretical predictions

To facilitate interpretation of the meta-analysis results, we first derived theoretical predictions for trait cline parallelism between ranges for a set of quantitative traits affecting local adaptation. The main results of our analysis, which build upon classic cline models from García-Ramos and Kirkpatrick [28], are summarized below and extended results are provided in the Supporting Information (SI). Following García-Ramos and Kirkpatrick [28], we assume that the optimum of each trait changes linearly across continuous geographic gradients (e.g., latitude) in the native and introduced ranges of a species. Conditions in the native range are sufficiently stable that native-range populations are locally adapted and at equilibrium between local selection and gene flow. Introduced range populations are initially displaced from equilibrium and gradually adapt to local conditions in the new range. For simplicity, we assume that species' range expansions across the introduced range are rapid relative to the tempo of local adaptation. Consequently, local adaptation primarily occurs *after* rather than during the

species' range shift. Nevertheless, clines emerging during the range shift—including drift-induced clines [21]—are incorporated into our analysis as initial conditions in the introduced range. From these initial conditions, which represent the state of introduced populations upon the completion of the range expansion, introduced clines subsequently evolve deterministically under the processes of local selection and gene flow.

Beginning with a single trait, let B_N and B_I represent the rates of change (slopes) of the trait optima across the native and introduced ranges, respectively (see the dashed lines in Fig. 1A), whereas b_N and b_I represent cline slopes of the trait (solid curves in Fig. 1A). Following García-Ramos and Kirkpatrick [28], we assume the trait is normally distributed with unit variance at each location in a range, and the trait heritability is constant across each range. Local selection is a Gaussian function of the trait value, with the optimum changing across each range and the strength of stabilizing remaining constant. With strong local selection relative to gene flow, equilibrium trait clines closely track the optimum. The native range cline is approximately $b_N = B_N$ (see Fig. 1A), while the introduced range cline is approximately:

$$b_{I,t} = B_I(1 - (1 - h^2\gamma)^2) + b_{I,0}(1 - h^2\gamma)^t \quad (1)$$

(SI Appendix 1), where h^2 is the trait's heritability, γ is the strength of stabilizing selection, t is the number of generations since the range expansion, and $b_{I,0}$ the initial trait cline slope immediately following the range expansion (the slope at time $t = 0$). The ratio of trait cline slopes over time is therefore $b_{I,t}/b_N \approx b_{I,t}/B_N$. If the initial cline in the introduced range is small relative to the native range cline (i.e., $|B_N| \gg |b_{I,0}|$), then the ratio of introduced to native range trait cline slopes will be nearly zero shortly after the range expansion (e.g., $b_{I,t}/b_N \approx 0$ when t is small; see Fig. 1A) and then converge over time to $b_I/b_N = B_I/B_N$, with the ratio eventually reflecting the similarity of local selection between the ranges.

Perfect parallelism of trait clines is expected at equilibrium if spatial changes of the optima are identical between ranges (at equilibrium, $b_I/b_N = 1$ when $B_I = B_N$) and all else is

equal (but note that differences between ranges in gene flow, trait heritability, or the strength of selection, can lead to persistently unequal cline slopes; see SI Appendix 2). ***Partial parallelism*** is expected when geographic shifts in the trait optima occur in the same direction in each range but differ in magnitude (i.e., $b_I/b_N > 0$ and $b_I/b_N \neq 1$, at equilibrium, if $B_I/B_N > 0$ and $B_I/B_N \neq 1$). ***Antiparallelism*** (i.e., "counter-clines", where $b_{I,t}/b_N < 0$) can occur in non-equilibrium populations when clines arise by drift during the range expansion (see [21]) or from indirect responses to selection on genetically correlated traits (see SI Appendix 6; for similar concepts but somewhat different terminology, see [29]). However, at equilibrium, counter-clines are only expected when trait optima shift in opposite directions between the ranges (B_I and B_N have opposite signs). Overall, a strong empirical pattern of parallelism is eventually expected (i.e., in sufficiently old introductions) when patterns of spatially varying selection are similar between native and introduced ranges. Deviations from perfect parallelism can arise from evolutionary lags to the equilibrium in the introduced range, divergent patterns of selection between ranges, or systematic differences between ranges in genetic or demographic constraints to local adaptation (SI Appendix 2; also see [21,28,30]).

Organisms are, of course, comprised of many traits that collectively respond to selection, leading to multivariate clinal divergence. Multivariate parallelism between ranges of a species can be quantified by comparing vectors of trait cline slopes from each range (Fig. 1B). Letting $\boldsymbol{b_I} = (b_{I,1}, b_{I,2}, \dots, b_{I,n})$ and $\boldsymbol{b_N} = (b_{N,1}, b_{N,2}, \dots, b_{N,n})$ represent the introduced- and native-range vectors of cline slopes for a common set of *n* traits, the total amount of clinal divergence in each range is captured by the Euclidean norms of the vectors ($\|\boldsymbol{b_I}\| = \sqrt{\sum_{i=1}^{n} b_{I,i}^2}$ and $\|\boldsymbol{b_N}\| = \sqrt{\sum_{i=1}^{n} b_{N,i}^2}$) and alignment of the multivariate orientations of clinal divergence in each range, as captured by the cosine of the angle between their cline vectors:

$$\cos(\theta) = \frac{\sum_{i=1}^{n} b_{I,i} \cdot b_{N,i}}{\|\boldsymbol{b_I}\| \cdot \|\boldsymbol{b_N}\|} \tag{2}$$

(see Fig. 1B), where $\cos(\theta) = 1$ indicates perfect alignment of cline orientations, $0 < \cos(\theta) < 1$ indicates partial alignment, and $\cos(\theta) < 0$ indicates strong misalignment between the ranges. Perfect parallelism between ranges occurs when $\|\boldsymbol{b_I}\|/\|\boldsymbol{b_N}\| = \cos(\theta) = 1$, and deviations from perfect parallelism can occur when ranges differ in their magnitudes and/or orientations of clinal divergence ($\|\boldsymbol{b_N}\| \neq \|\boldsymbol{b_I}\|$ and/or $\cos(\theta) < 1$).

What patterns of multivariate parallelism should we expect when native and introduced ranges span similar environmental conditions? If traits contributing to local adaptation are genetically independent of one another, local selection is strong relative to gene flow, and trait clines are initially absent following the range expansion ($b_0 = 0$ for each trait), then the model makes three predictions (see SI Appendix 3 and the broken lines in Fig. 1C). First, none of the traits will show counter-clines between ranges ($b_{I,t}/b_N \geq 0$ for all traits at all times). Second, the ratio of cline magnitudes shows a strong increase over time, with an initial value of $\|\boldsymbol{b_I}\|/\|\boldsymbol{b_N}\| = 0$ and a final value of $\|\boldsymbol{b_I}\|/\|\boldsymbol{b_N}\| \approx 1$ if changes in the trait optima are the same between ranges (or more generally, $\|\boldsymbol{b_I}\|/\|\boldsymbol{b_N}\| \approx \sqrt{\mathrm{var}(B_I) + \bar{B}_I^2}/\sqrt{\mathrm{var}(B_N) + \bar{B}_N^2}$ at equilibrium, with $\bar{B}_I$, $\bar{B}_N$, $\mathrm{var}(B_I)$ and $\mathrm{var}(B_N)$ representing the means and variances of optimum slopes of the ranges). Third, the alignment of cline vectors increases from an initial value of $\cos(\theta) \approx \cos(\theta_{eq.})/\sqrt{1 + \mathrm{var}(h^2\gamma)/\left(\overline{h^2\gamma}\right)^2}$ to an equilibrium value of $\cos(\theta_{eq.})$, where $\mathrm{var}(h^2\gamma)$ and $\overline{h^2\gamma}$ represent the mean and the variance (among traits) for the compound parameter $h^2\gamma$. Variation in $h^2\gamma$ causes heterogeneity among traits in the rate at which they respond to selection, which dampens the initial alignment of clinal divergence between the ranges relative to the alignment at equilibrium. However, this effect is usually small and the total change in $\cos(\theta)$ over time is, therefore, small relative to the total change in $\|\boldsymbol{b_I}\|/\|\boldsymbol{b_N}\|$.

These three predictions change substantially if drift-induced clines occur during the range expansion. If clines evolve under pure drift during the range expansion (as in [21]), then their slopes may reasonably be approximated as normally distributed with mean of zero and variance (denoted $\mathrm{var}(b_{I,0})$) determined by the demography of the range expansion and the heritability of the trait (see SI Appendix 4). While we do not explicitly model the formation of clines by drift, the phenomenon is easily incorporated into our model by exploring how different values of $\mathrm{var}(b_{I,0})$ affect the temporal patterns of multivariate parallelism between ranges (SI Appendix 5). Returning to our model of genetically independent clines (as above), we find that drift-induced clines, firstly, generate a high proportion of counter-clines between ranges involving recent introductions (~50% of traits, initially; Fig. 1C, bottom panel). This proportion then declines over time as introduced populations locally adapt to environmental conditions that parallel those in the native range. Second, drift clines can lead to substantial clinal divergence in recent introductions (e.g., the solid grey curve in Fig. 1C, top panel, where the initial ratio of magnitudes is $\|\boldsymbol{b_I}\|/\|\boldsymbol{b_N}\| \approx \sqrt{\mathrm{var}(b_{I,0})/\mathrm{var}(B_N)}$; see SI Appendix 5). In such cases, the ratio of cline magnitudes may show relatively modest change over time. Third, the alignment between native and invasive trait cline orientations dramatically shifts over time, from initially no alignment ($\cos(\theta) = 0$) to strong alignment at equilibrium (e.g., $\cos(\theta) = 1$ at equilibrium when environmental conditions are identical between the ranges, the solid black curve in Fig. 1C, top panel). Consequently, the total change in $\cos(\theta)$ over time can be much greater than the change in $\|\boldsymbol{b_I}\|/\|\boldsymbol{b_N}\|$. Similar patterns can occur when there are genetic correlations between traits, which can lead to counter-clines for individual traits and (depending on the timescale) a greater change in $\cos(\theta)$ than in $\|\boldsymbol{b_I}\|/\|\boldsymbol{b_N}\|$ (see SI Appendix 6).

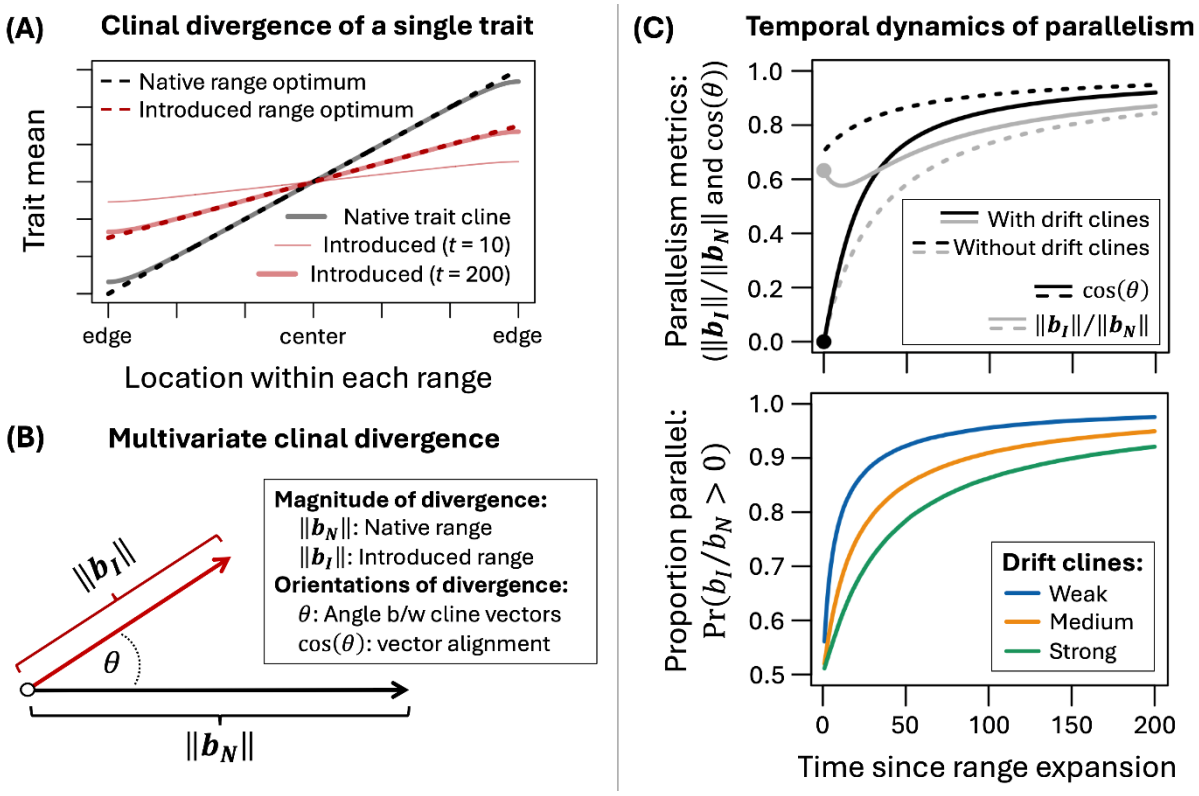

Figure 1. Theoretical predictions for parallelism of trait clines between ranges. **Panel A:** Examples of single trait clines in a native (black) and introduced range (red). The native range trait cline is evaluated at equilibrium, while the introduced trait cline is evaluated after $t = 10$ and $t = 200$ generations following the range expansion. Selection for local adaptation is assumed to be strong relative to the swamping effects of gene flow, leading to a close match between trait clines and optima at equilibrium (see SI Appendix 1). Extensions of the model and further results are presented in SI Appendix 1-2. **Panel B:** Metrics of multivariate trait clines across the native and introduced range. The lengths of black and red arrows show the magnitudes of clinal divergence in the native and introduced ranges, respectively. The angle between cline slope vectors ($0 < \theta < \pi$) and cosine of the angle ($-1 < \cos(\theta) < 1$) measure the degree of divergence and alignment (respectively) between the cline orientations in each range (see the text for elaboration). **Panel C:** Evolution of increased parallelism between native and introduced ranges that span similar environmental conditions. The top panel shows the tempo of convergence between ranges for the magnitudes and orientations of native and introduced trait cline vectors ($\|\boldsymbol{b_I}\|/\|\boldsymbol{b_N}\|$ and $\cos(\theta)$ approach one over time). The bottom panel shows the proportion of traits exhibiting parallel clines between ranges (the proportion of traits with $b_I/b_N > 0$, as opposed to counter-clines, where $b_I/b_N < 0$). Native range clines are at migration-selection equilibrium, while introduced clines gradually evolve towards equilibrium following the range expansion. Total clinal divergence is determined by many genetically independent traits ($n = 10^5$), with the product of heritability and stabilizing selection for each trait ($h^2\gamma$) drawn from an exponential distribution with mean of 0.02. Cline optimum slopes for the traits follow a standard normal distribution, assumed here to be identical between ranges, which leads to perfect parallelism at equilibrium ($\|\boldsymbol{b_I}\|/\|\boldsymbol{b_N}\| = \cos(\theta) = 1$ with large t).

Genetic drift during the range expansion generates nonzero initial cline slopes (see [21]). The top panel compares the dynamics of parallelism with strong drift-induced initial trait clines (solid curves, where $\mathrm{var}(b_{I,0}) = 0.4\,\mathrm{var}(B_N)$) versus parallelism without drift-induced clines (broken curves, where $b_{I,0} = 0$). The grey and black circles show the predicted initial states with drift clines: $\|\boldsymbol{b_I}\|/\|\boldsymbol{b_N}\| \approx \sqrt{\mathrm{var}(b_{I,0})/\mathrm{var}(B_N)}$ and $\cos(\theta) \approx 0$ (SI Appendix 5). The bottom panel shows three degrees of drift-induced clines: weak drift clines ($\mathrm{var}(b_{I,0}) = 0.01\,\mathrm{var}(B_I)$), medium drift clines ($\mathrm{var}(b_{I,0}) = 0.1\,\mathrm{var}(B_I)$), and strong drift clines ($\mathrm{var}(b_{I,0}) = 0.5\,\mathrm{var}(B_I)$)).

Methods

Meta-analysis data

We compiled the meta-analysis data following PRISMA guidelines ([31]; see SI Fig. S1), and included studies reporting trait clines in both the native and introduced ranges of the study species. Eligible articles were identified from searches of Web of Science, Scopus, and PubMed (initial searches were carried out in December 2022 and repeated in May 2025). Keywords were a combination of synonyms related to clines (e.g., "clinal variation"), introduced species (e.g., "introduced"), plant (e.g., "weed"), and the term "adapt*" (see SI Fig. S1 for details). We included studies using common garden experiments published in academic journals with titles and abstracts in English. Studies cited in identified articles were added to our database if they met the inclusion criteria.

When possible, we obtained raw data published online or provided by authors. When raw data were not available, we extracted mean trait values and standard errors from figures using ImageJ [32]. Studies with less than four populations were excluded from the analysis. We also excluded studies focusing on 'expanded' ranges, where the native range has recently expanded within the same continent [33]. A total of 34 studies met our inclusion criteria (SI Box S1). Some studies grew plants under multiple common garden treatments (e.g., different water or nutrient regimes) or implemented common garden experiments at different sites. These "experiments" were analyzed separately because trait values could not be directly

compared across experiments. When multiple introduced ranges were tested against a single native range, we considered each pair of contrasts as a separate "experiment". The final dataset includes paired (native and introduced) cline estimates for 465 traits, from 86 experiments, spanning 23 species and 10 plant families (SI Table S1). Each trait was classified into one of the following categories (SI Table S2): morpho-physiology (structural features and functional processes), reproduction (investment in offspring production), size (biomass and growth traits), phenology (timing of developmental stages) and defense (physical and chemical traits that resist herbivory).

Estimation of the number of generations since introduction

To estimate species' introduction times, we used the year of introduction to the study area when it was provided by authors. When that information was not available, we used the first record of introduction reported by Seebens *et al*. [34], for countries matching the source populations of each species in our dataset. When records for the source country were unavailable, we used records from the closest country on the same continent. For studies involving populations sampled from multiple countries, we used the average year of the first record across the countries. Years since introduction were calculated as the year of seed collection minus the year of first record. When seed collection dates were not available, we used the year of the common garden experiment. The number of generations since introduction was calculated as [years since introduction]/[generation time], with species' generation times (in years) obtained from [35]. When generation time data were not available, we approximated generation time as $T_z = \alpha + 0.5(\omega - \alpha)$, where α is the species' age at reproductive maturity and ω is the typical lifespan [36], each obtained from the TRY database [37]. With accurate measures of α and ω, T_z provides a good approximation of generation time [38].

Effect size calculations

All statistical analyses were performed with the R software v 4.4.1 [39] .

Estimation of individual trait cline slopes

For each experiment, we estimated cline slopes using linear models with the population-level trait means as the response variable and the environmental gradient the authors of the original studies focused on as the explanatory variable. These environmental gradients included latitude, principal components of BioClim data, temperature, elevation, aridity, altitude, and longitude. We also analyzed the data using a single shared environmental predictor across the set of experiments (e.g., absolute latitude, temperature, or precipitation, with the latter two predictors calculated following Atwater *et al*. [40]). Within each experiment, traits were standardized (mean = 0; standard deviation = 1) across both native and introduced populations before model fitting. Traits with highly skewed distributions were square root or log transformed prior to standardization to improve residual normality. For each trait, population means were used to obtain a native slope (b_N), an introduced slope (b_I), and their standard errors.

Multivariate parallelism

We estimated multivariate parallelism in 73 experiments with more than one trait. For each experiment, we compiled vectors of trait cline estimates for the introduced and native range ($\boldsymbol{b_I}$ and $\boldsymbol{b_N}$), from which we calculated vectors norms ($\|\boldsymbol{b_I}\|$ and $\|\boldsymbol{b_N}\|$) and the cosine similarity between vectors ($\cos(\theta)$) using eq. (2) (also see [41,42]). We analyzed log-transformed ratio of magnitudes, $\ln(\|\boldsymbol{b_I}\|/\|\boldsymbol{b_N}\|)$, where $\ln(\|\boldsymbol{b_I}\|/\|\boldsymbol{b_N}\|) = 0$ indicates equal magnitudes between ranges.

Uncertainty around the point estimates of $\cos(\theta)$ and $\ln(\|\boldsymbol{b_I}\|/\|\boldsymbol{b_N}\|)$ was estimated by bootstrapping the original data by randomly selecting individual samples with replacement.

For each bootstrapped sample, we used population means of trait values to calculate the parameters using the methods described above. In cases where only the population means and standard errors were available (but not raw data), we simulated trait means for each population by pseudo-random sampling from a normal distribution with the mean corresponding to the point estimate of the mean for the population and standard deviation corresponding to its standard error. Each set of simulated means across populations within a range was used to calculate cline slopes, from which we recalculated multivariate parameters of parallelism. We repeated this process 10,000 times to approximate confidence intervals for these parameters.

Univariate parallelism

Our univariate analysis focused on traits with statistically significant clines in at least one range (251 of 465 traits in the dataset), as those without a significant cline in either range are irrelevant to tests of parallelism (Fig. 3). We used ratios of cline slopes (i.e., b_I/b_N) because they facilitate comparisons of effect sizes between the wide assortment of traits and study systems in the dataset, regardless of the original units of measurement of the traits or the environmental gradients chosen by the authors. Following Friedrich *et al*. [43], we calculated the relative magnitudes of univariate clinal divergence using the natural logarithm of cline slope ratios ($\ln(b_I/b_N)$), which allows parametric statistical analyses of meta-analysis effect sizes. 95% confidence intervals for the mean $\ln(b_I/b_N)$ of each trait were calculated using equations presented by Friedrich *et al*. [43].

Meta-analysis

Overview

Meta-analyses were performed using the function *rma.mv* from the package 'metafor' [44]. Parameters in the meta-analytical models were estimated using restricted maximum likelihood

[45], with Knapp-Hartung adjustments used to calculate the confidence interval of pooled effects [46]. We performed multilevel random-effects models to account for the hierarchical structure of non-independence in our dataset (multiple traits in multiple experiments within single studies; multiple studies examine the same species). We used the function *var.comp* from the package 'dmetar' [47] to calculate the total heterogeneity (I^2), and heterogeneity at each level ($I^2_{\text{level 2}}$ and $I^2_{\text{level 3}}$). We tested whether residual heterogeneity was due to sampling error only, using the QE statistic, with significant QE indicating that residual heterogeneity can be explained by factors not included in the model [44].

Multivariate analysis

The meta-analysis of multivariate parameters estimated pooled effect sizes and 95% confidence intervals for $\cos(\theta)$ and $\ln(\|\boldsymbol{b_I}\|/\|\boldsymbol{b_N}\|)$, with random effects of study identity nested within a species. We tested for relationships between multivariate parameters and the number of generations since introduction by including generations since introduction, the number of traits included in each experiment, and their interaction as moderators. We used the function *glmulti* (package 'glmulti' [48]) to select the best model based on Akaike information criterion with small sample size correction (AICc). Models within ΔAICc < 2 were considered competitive [49], and we compared the model-averaged importance of each term within the competitive model set to determine the final model structure.

Univariate analysis

Before performing the formal meta-analysis, we first tested whether the proportion of clines going in the same direction ($b_I/b_N > 0$) changed with the number of generations since introduction (as predicted by theory; Fig. 1C). We built a generalized linear model (*glm*) with

generations-since-introduction as the fixed effect, a binomial error distribution and a logit link function, and a binary response variable (0 = [b_I/b_N <0] and 1 = [b_I/b_N > 0]).

The subsequent univariate meta-analysis focused on positive ratios of clines (traits where $b_I/b_N > 0$), which indicate parallelism in a true sense and because logarithm is defined in such cases (we note that analyses of the absolute value of b_I/b_N, using the full set of clines that include $b_I/b_N < 0$ and $b_I/b_N > 0$, yield qualitatively similar patterns of relative cline magnitudes between native and introduced ranges, Fig. S3). The model included random effects of experiment identity, nested within the study identity, accounting for within- and between-study heterogeneity. Species identity was not included in the model because the multivariate analysis revealed little heterogeneity explained by species identity (analyses with species identity included did not change the results). Following the same method as before, we examined how trait category, generations-since-introduction and their interaction affected the extent of parallelism between native and introduced ranges. The package 'orchaRd' was used for graphical purposes [50].

We also conducted the same univariate analysis of estimated slopes using a composite trait value extracted using a principal component analysis (PCA) within each experiment. We conducted a PCA using *princomp* function from the package 'stats', with a dataset including a full set of all traits investigated by authors. The cline slope for the first principal component (trait PC1) against environmental gradients was estimated for native and introduced ranges as above.

Results

Multivariate analysis of clinal divergence

We found that the alignment of native and introduced range vectors ($\cos(\theta)$) was positive in 62% (46 of 74) of experiments ($\chi^2 = 1.7, P = 0.19$). The mean alignment between native and

introduced cline vectors was 0.31 ([0.14, 0.49], t_{73} = 3.6, P = 0.0005), which indicates partial alignment between native and introduced clines. The average log ratio of cline vector magnitudes (the mean of $\ln(\|\boldsymbol{b_I}\|/\|\boldsymbol{b_N}\|)$) was -0.30 ([-0.58, -0.02], t_{73} = 2.2, P < 0.0001, Fig. 2A), which indicates that introduced populations tend to have shallower clines (74% of native cline magnitudes, on average). Residual heterogeneity (i.e., QE) was significant, primarily due to study identity in both metrics (SI Table S3).

Variation in vector alignment was best explained by the effect of generations since introduction, with $\cos(\theta)$ increasing with introduction time (*slope* = 0.004, t_{72} = 3.0, P = 0.0037, Fig. 2B, SI Table S4). In contrast, $\ln(\|\boldsymbol{b_I}\|/\|\boldsymbol{b_N}\|)$ did not correlate with generations since introduction (*slope* = 0.0021, t_{72} = 1.1, P = 0.29, Fig. 2C), nor did any other effect. These results indicate that the increase in parallelism with time since introduction is primarily due to improved alignment of cline orientations rather than changes in the relative magnitudes of multivariate clinal divergence between ranges.

The results summarized above are for clines associated with the spatial or environmental gradients chosen by authors of the original studies. To evaluate the robustness of these results, we repeated the multivariate analyses using re-estimated trait clines predicted by absolute latitude, or gradients in temperature or precipitation. Results for $\cos(\theta)$ and $\|\boldsymbol{b_I}\|/\|\boldsymbol{b_N}\|$ were similar for each predictor of clinal divergence, though clines across precipitation gradients resulted in quantitatively weaker degrees of parallelism relative to other gradients (SI Table S5). Associations with time since introduction remained significantly positive for latitudinal clines, but not for clines predicted by temperature or precipitation gradients (SI Table S6).

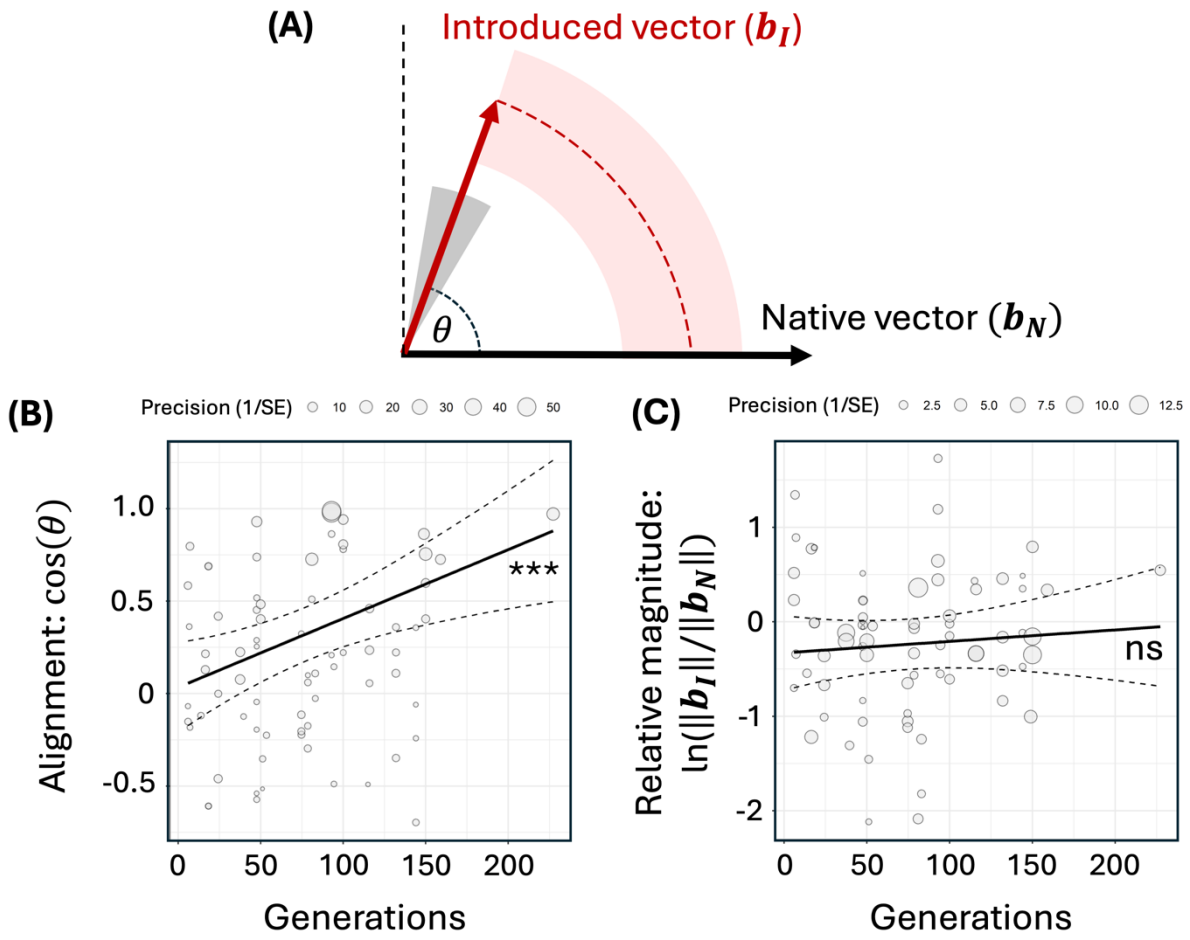

Figure 2. Multivariate clinal divergence between introduced and native ranges. **Panel A** shows cline vectors of native and introduced ranges are presented as arrows (black and red, respectively), with the angle between the vectors (θ) indicating the mean degree of divergence between the orientations of native and introduced trait cline vectors. The length of the introduced vector represents the mean magnitude of introduced vector relative to that of the native vector ($\|\boldsymbol{b_I}\|/\|\boldsymbol{b_N}\|$), where the native vector magnitude is scaled to one ($\|\boldsymbol{b_N}\| = 1$). Grey shading denotes the 95% CI of θ, and pink shading denotes the 95% CI of $\|\boldsymbol{b_I}\|/\|\boldsymbol{b_N}\|$. **Panels B and C** show associations between the number of generations since introduction and **(B)** cos(θ) or **(C)** ln($\|\boldsymbol{b_I}\|/\|\boldsymbol{b_N}\|$), with meta-analytic data shown as bubble plots. Asterisks indicate a significant association with time (*** $P < 0.0001$).

Univariate analysis of divergence across different trait categories

Among the 251 trait pairs with a significant cline in at least one range (Fig. 3), 58% of traits (145 of 251) had the same direction in each range ($b_I/b_N > 0$) and the rest had opposite directions ($b_I/b_N < 0$). The proportion of clines that diverged in the same direction increased with the number of generations since introduction (*slope* = 0.010, z = 3.6, P = 0.0003; see Fig. 4A).

This pattern holds qualitatively for each trait category and trait PC1 analyzed separately, though interactions with time were only significant for the size-related traits (SI Fig. S2), possibly owing to the smaller sample sizes of other trait categories.

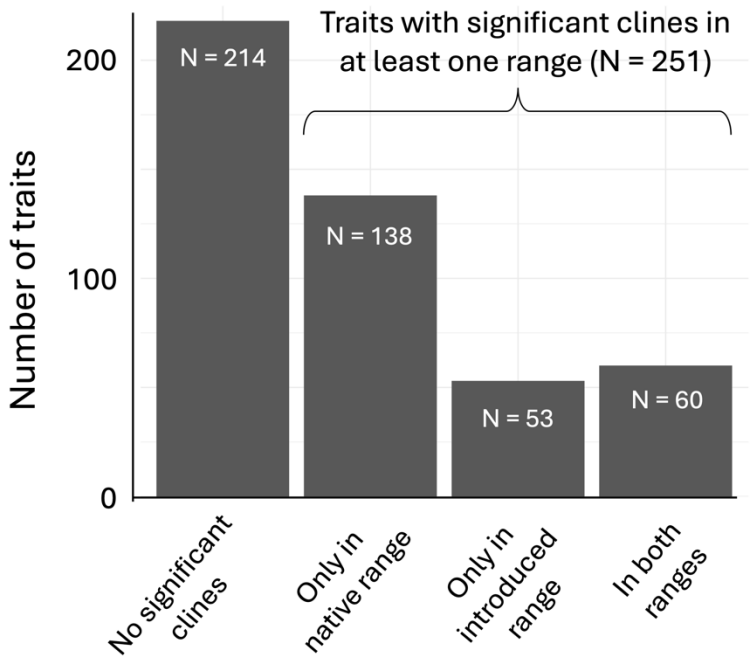

Figure 3. Results of the linear model tests for clinal variation in 465 traits of the meta-analysis. Slope estimates were (left to right): non-significant in both ranges, significant in the native range only, significant in the introduced range only, or significant in both ranges.

For the subset of clines with the same sign (those with $b_I/b_N > 0$), native clines were, on average, steeper than introduced clines, with the magnitude of introduced clines being 77% of their native counterparts (mean $\ln(b_I/b_N)$ = -0.26, 95% CI = [-0.51, -0.01]). Residual heterogeneity (i.e., QE) was significant, primarily due to study identity (SI Table S3).

Variability in $\ln(b_I/b_N)$ was not associated with the time since introduction (*slope* = -0.0001, t = 0.0019, P = 0.98; Fig. 4B). Instead, the variability was best explained by trait category alone (SI Table S4). The magnitude of clinal divergence was similar between ranges for defense and reproductive traits, with introduced clines showing 89% and 111% the magnitude of native clines, respectively ($\ln(b_I/b_N)$ = -0.11 [-0.73, 0.50] and $\ln(b_I/b_N)$ = 0.10 [-

0.22, 0.43]). In contrast, introduced clines were systematically shallower than native clines for morpho-physiology (64%, $\ln(b_I/b_N)$ = -0.45 [-0.88, -0.02]), phenology (71%, $\ln(b_I/b_N)$ = -0.35 [-0.66, -0.04]), and size traits (70%, $\ln(b_I/b_N)$ = -0.36 [-0.66, -0.06]) (Fig. 4C). The magnitude of divergence in trait PC1 was similar between ranges, with introduced clines showing 94% of native clines ($\ln(b_I/b_N)$ = -0.06 [-0.42, 0.29]).

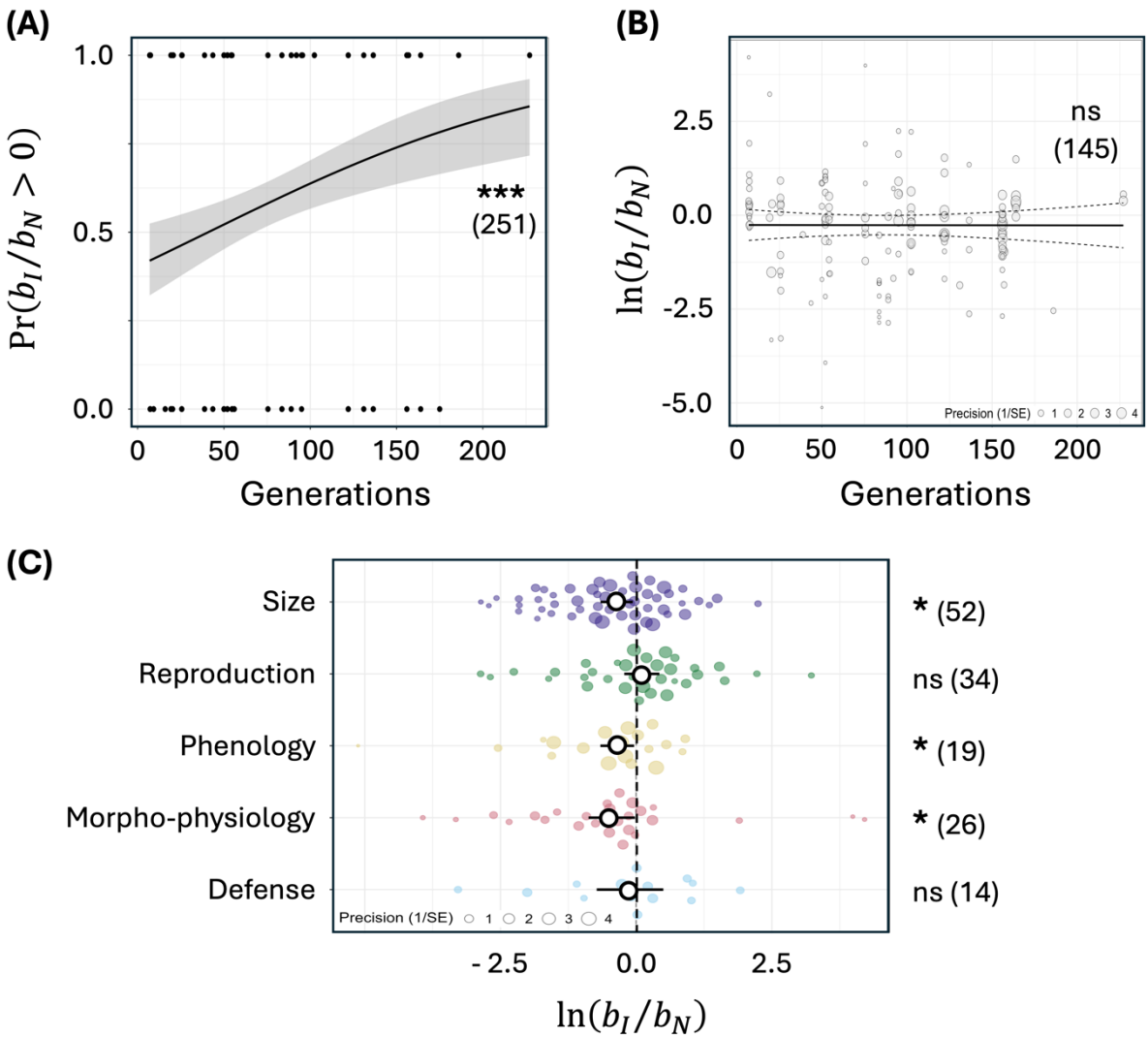

Figure 4. Univariate estimates of parallelism between native and introduced ranges. **Panels A-B** show the relationship between the number of generations since introduction and **(A)** the probability that clines in each range diverge in the same direction (i.e., $b_I/b_N > 0$, analyzed using a generalized linear model), or **(B)** the relative magnitude of cline slopes in each range ($\ln(b_I/b_N)$, calculated for traits where $b_I/b_N > 0$). **Panel C** shows $\ln(b_I/b_N)$ values for the same set of traits as in **(B)**, but analyzed separately for each trait category. Mean effect sizes in **(C)** (white circles) are plotted with 95% confidence intervals (bold

line), with the number of traits given in brackets (SI Table S7). Asterisks indicate significant deviations from $\ln(b_I/b_N) = 0$ (perfect parallelism). Individual effect sizes (colored circles) for the five trait categories are plotted with circle size denoting precision (inverse variance). Asterisks indicate a significant association with time. * $P < 0.05$.

Discussion

Our meta-analysis reveals three broad patterns of evolutionary parallelism between the trait clines of native versus introduced ranges. First, multivariate parallelism across the entire dataset is relatively low, on average, owing to shallower magnitudes of clinal divergence in introduced relative to native ranges (mean $\|\boldsymbol{b_I}\|/\|\boldsymbol{b_N}\| \approx 0.73$) and modest alignment of cline directions between ranges (mean $\cos(\theta) \approx 0.30$). Second, multivariate parallelism between ranges markedly increases with the residence time of introduced populations (generations since introduction), resulting in strong parallelism between ranges involving relatively old introductions (i.e., the linear model predicts that $\|\boldsymbol{b_I}\|/\|\boldsymbol{b_N}\|$ and $\cos(\theta)$ both approach one at 200 generations post introduction, though the increase in $\|\boldsymbol{b_I}\|/\|\boldsymbol{b_N}\|$ is not statistically significant; see Fig. 2B). This increase in parallelism over time is primarily caused by increased alignment of cline directions between ranges (increased $\cos(\theta)$) rather than changes in relative cline magnitudes. Third, degrees of parallelism between ranges vary among traits, and are stronger for reproductive and defense traits than for phenological, morpho-physiological, and size-related traits; the latter three categories exhibit weaker clines in introduced ranges. Below, we discuss processes that might explain these observations before outlining opportunities for future work.

Factors affecting the relative magnitudes of trait clines in native and introduced ranges

Several evolutionary mechanisms could contribute to shallower clines in introduced relative to native ranges (*i.e.*, $\|\boldsymbol{b_I}\|/\|\boldsymbol{b_N}\| < 1$). Most notably, shallower clines in introduced ranges are expected when there are time lags in local adaptation and introduced populations are still in the

process of adapting to environmental conditions across their new ranges [51]. On the one hand, the time-lag hypothesis predicts that the ratio of cline magnitude in introduced versus native ranges ($\|\boldsymbol{b_I}\|/\|\boldsymbol{b_N}\|$) should increase with the residence time of introduced populations, yet our compiled estimates of $\|\boldsymbol{b_I}\|/\|\boldsymbol{b_N}\|$ showed, at best, a weak (and non-significant) increase with residence time (see Fig. 2C). Similarly weak interactions with time were observed for univariate clines of different trait categories. On the other hand, such patterns are expected if trait clines initially arise by drift during range expansions and subsequently evolve in response to selection for local adaptation (see Fig. 1C). Drift-induced clines can emerge in recent invasive species by two different mechanisms: (1) multiple independent introductions at different locations in the new range, followed by incomplete mixing when populations contact [52] and (2) successive founder-effects during expansion following single introductions (see [21]). Further work is needed to test the extent to which nonadaptive clines arise in recent introductions, through experiments that control for effects of genetic ancestry from multiple introductions [52]. Time-series data (e.g., from herbarium specimens) may also show that early mismatches between ranges are later resolved as introduced populations evolve clines that better match native clines (e.g., the hb-chr5b haplotype in common ragweed [27]). Similarly, spatial sorting of dispersal-related traits during expansion, documented in both plants and animals (see [53,54]), can create gradients that are potentially correlated with environmental variables but primarily reflect colonization history rather than local adaptation.

Differences between ranges in the steepness of environmental gradients represent an additional factor potentially causing differences in native and introduced trait clines. Shallower clines in the introduced range are expected, even at equilibrium, in cases where environmental gradients are shallower in the introduced compared to the native range. Trait clines might be shallower on average in introduced ranges if species are disproportionately introduced into geographic regions where the environmental gradients are relatively shallow, which would

facilitate range expansions in those regions [55]. For example, urban environments that many invasive plants occupy [56] may provide more homogeneous landscapes than natural systems [57]. Unfortunately, direct comparisons of environmental gradients between native and introduced ranges are lacking, making it difficult to formally evaluate this hypothesis.

A more complex picture emerges in the presence of genetic, evolutionary, and demographic factors that constrain local adaptation, potentially leading to shallower clines in introduced ranges (see SI Appendix 2). For example, weaker selection and/or lower genetic variation in introduced ranges would enhance the swamping effects of gene flow on clinal divergence, resulting in shallower clines at migration-selection balance. Heritability estimates [58–62] and linear selection gradients [21] were each found to have similar magnitudes between native and introduced ranges, which offers little support for this possibility, though such data are admittedly sparse and the hypothesis deserves further attention. Demographic differences between ranges—including differences in the rate of dispersal or the spatial distribution of population density (see SI Appendix 2)—can also lead to different degrees of swamping of local adaptation between ranges. Invasive herbaceous plant species tend to have higher dispersal rates than non-invasive ones [63], and increased dispersal ability can evolve within introduced ranges [58,64], which could lead to higher swamping by gene flow in introduced ranges relative to native ranges. The distribution of population density affects local adaptation by mediating the rate of gene flow from the center of a range to its edges (see SI Appendix 2; [28]). If, for example, introduced range populations more closely conform to an "abundant-center" distribution than native range populations (which might be likely in actively expanding introductions; [65]) they will be more susceptible to swamping and evolve shallower clines.

The trend towards shallower clines in introduced ranges does not, however, apply across the board. Defense and reproductive traits have similar cline magnitudes between

ranges, while clines for phenological, morpho-physiological, and size-related traits were shallower (roughly half as steep) in introduced relative to native ranges. These differences among trait categories might stem from differences in evolutionary potential for rapid local adaptation, with traits under exceptionally strong selection or with high heritabilities evolving more rapidly in introduced ranges. Reproductive traits, for example, are thought to be under strong selection because they are closely related to fitness [66,67]. Likewise, the average heritability of plant secondary metabolites (which includes defensive compounds) is estimated to be more than twice as large as the heritability of phenological, morphological, physiological, and size traits, which should facilitate strong responses to selection ([68]; see also [58,69]).

Factors affecting the alignment of cline directions between ranges over time

Four factors potentially contribute to the weaker alignment of cline directions in more recent than older introductions (recall that $\cos(\theta)$ quantifies alignment between ranges). First, traits differ in how responsive they are to natural selection: those with high heritability and under strong selection will rapidly adapt to local conditions across the new range, while those with low heritability or weak selection should exhibit protracted lags in local adaptation (see the SI Appendix 2). This heterogeneity of lag-times among traits leads to temporary misalignments in the relative magnitudes of clines in each range, which eventually resolve as each trait evolves to migration-selection equilibrium in the new range (see the black broken curve in Fig. 1C).

Second, drift-induced clines that emerge at the outset of a range expansion can strongly depress the initial alignment of clinal divergence between ranges. For example, if introduced clines initially arise by drift during the range expansion, then the alignment of clines between ranges will initially be poor ($\cos(\theta) \approx 0$ initially) with a large proportion of traits showing counter-clines (Fig. 1C). If selection pressures are similar between ranges, stochastic and historical effects on the initial formation of clines are expected to diminish over time, as natural

selection reorients clines to align with those maintained in the native range, leading to the observed increase in parallelism among the older introductions.

Third, strong genetic correlations between traits can also generate transient counter-clines in traits subject to relatively weak selection (see SI Appendix 6). Strong parallelism of clines (e.g., $\|\boldsymbol{b_I}\|/\|\boldsymbol{b_N}\| \approx \cos(\theta) \approx 1$) can ultimately evolve between the native and introduced ranges, yet strong genetic constraints can draw out this process, leading to extended lags in local adaptation of introduced populations and extensive change in the alignment of selection over time. Strong genetic correlations and trade-offs between fitness-related traits may indeed be common. For example, both early flowering and large biomass (and seed production) are favored at high latitudes, yet these traits negatively covary, providing the potential for the evolution of transient counter-clines in the more weakly selected trait (see [19,70]).

Fourth, the directions of selection in each range might change over time, leading to a greater alignment of both selection and trait clines in old relative to recent introductions. For example, selection may fundamentally differ between recent and old introductions if the former experiences a release from natural enemies, but the latter does not. Enemy release might relax selection of defense traits within the new range and facilitate evolution of defense trait clines caused by drift or by indirect responses to selection of genetically correlated traits (as predicted by the "evolution of increased competitive ability" (EICA) hypothesis [71]). Moreover, relaxation of herbivory may alter the pattern of selection on secondary metabolites with dual functions in herbivore defense and abiotic stress tolerance [25], with metabolite concentrations in recently introduced species evolving in response to selection for abiotic stress tolerance rather than herbivore defense [25]. Clines favored by selection in recent introductions may, thus, differ substantially from those in the native range. However, subsequent accumulation of natural enemies in the introduced range over time [72,73] may gradually reshape the selective

landscapes of older introduced ranges, leading to a stronger alignment of selection and evolutionary parallelism of clines between native and introduced ranges.

Conclusions and future directions

A trait or allele frequency cline is not, in itself, evidence for local adaptation [21]. However, repeated evolution of parallel clines between geographically disjunct regions of a species' range is difficult to reconcile with nonadaptive explanations and is instead indicative of repeated local adaptation to shared environmental conditions between the regions [74,75]. We found that geographic clines in plant traits show strong evolutionary parallelism between native and introduced ranges with relatively long residence times (on the order of 100 or more generations). This result applies to a broad set of plant species and trait types and implies that local adaptation is extensive and predictable across native ranges and mature introduced ranges.

Our analysis suggests that the greater parallelism of older relative to more recent introductions is primarily due to an increase in the alignment of cline directions between ranges rather than changes to the relative magnitudes of clines in introduced versus native ranges—a pattern that holds qualitatively across different trait categories. Although several factors may contribute to this pattern, we suspect it is caused by rapid evolution of maladaptive clines in recent introductions—owing to processes like drift, founder effects, and spatial sorting during colonization (see Fig. 1C), or to indirect responses to selection of genetically correlated traits (see SI Appendix 6). This early stage of cline formation may then be followed, in the longer term, by more gradual evolution of local adaptation that increases parallelism between clines in each range. Direct tests for enrichment of maladaptive clines in recent relative to old introductions (e.g., through estimates of selection of clinally diverging traits) would, therefore, be a worthwhile focus for future work. Other potentially useful extensions of our study include analyses of nonlinear clines (which are sometimes reported in cline studies, e.g., [12,76]) and

their evolutionary parallelism between ranges, and analyses of the joint tempo of changes in trait clines and the geographic breadths of introduced species' ranges, both of which may increase over time, with adaptive clines possibly facilitating expansions of range breadth [55].

Finally, we used a snapshot of clinal divergence in species that differed in their arrival times into new ranges to indirectly infer temporal dynamics of cline evolution. However, a true time-series analysis of evolutionary parallelism between native and introduced clines would also be valuable, though such data are much more difficult to obtain. In a rare exception, Wu and Colautti [19] analyzed herbarium records to compare clinal patterns of flowering phenology in three introduced ranges of *Lythrum salicaria* over 150 years, and found lags in the evolution of adaptive clines in all three regions. Because herbarium specimens are collected in the field, the contribution of phenotypic plasticity to the trait variation must be controlled [19], although genomic analyses [27] or quantitative genetic approaches can be leveraged to overcome those issues [77]. It will be interesting to see how strongly true time-series analyses conform to the patterns of increasing parallelism implied by our study.

References

1. Arendt J, Reznick D. Convergence and parallelism reconsidered: what have we learned about the genetics of adaptation? Trends Ecol Evol. 2008;23: 26–32.
2. Stern DL. The genetic causes of convergent evolution. Nat Rev Genet. 2013;14: 751–764.
3. Gould SJ. Wonderful life: the Burgess Shale and the nature of history. WW Norton & Company; 1989.
4. Messer PW, Ellner SP, Hairston NG. Can population genetics adapt to rapid evolution? Trends Genet. 2016;32: 408–418.
5. Agrawal AA, Hastings AP, Johnson MTJ, Maron JL, Salminen J-P. Insect herbivores drive real-time ecological and evolutionary change in plant populations. Science. 2012;338: 113–116.
6. Gomulkiewicz R, Houle D. Demographic and genetic constraints on evolution. Am Nat. 2009;174: E218–E229.

7. Maynard Smith J. What determines the rate of evolution? Am Nat. 1976;110: 331–338.

8. Caruso CM, Martin RA, Sletvold N, Morrissey MB, Wade MJ, Augustine KE, et al. What are the environmental determinants of phenotypic selection? A meta-analysis of experimental studies. Am Nat. 2017;190: 363–376.

9. Siepielski AM, Morrissey MB, Buoro M, Carlson SM, Caruso CM, Clegg SM, et al. Precipitation drives global variation in natural selection. Science. 2017;355: 959–962.

10. Prentis PJ, Wilson JR, Dormontt EE, Richardson DM, Lowe AJ. Adaptive evolution in invasive species. Trends Plant Sci. 2008;13: 288–294.

11. Hodgins KA, Battlay P, Bock DG. The genomic secrets of invasive plants. New Phytol. 2025;245: 1846–1863.

12. van Boheemen LA, Atwater DZ, Hodgins KA. Rapid and repeated local adaptation to climate in an invasive plant. New Phytol. 2019;222: 614–627.

13. Maron JL, Vilà M, Bommarco R, Elmendorf S, Beardsley P. Rapid evolution of an invasive plant. Ecol Monogr. 2004;74: 261–280.

14. Etterson JR, Craig TP, Ohgushi T, Delf DE, Craig TP, Ando Y. Parallel patterns of clinal variation in *Solidago altissima* in its native range in central USA and its invasive range in Japan. Botany. 2008;86: 91–97.

15. Liu W, Chen X, Wang J, Zhang Y. Does the effect of flowering time on biomass allocation across latitudes differ between invasive and native salt marsh grass *Spartina alterniflora*? Ecol Evol. 2022;12: e8681.

16. Liu W-W, Zhang Y-H. Geographical variation in germination traits of the salt-marsh cordgrass *Spartina alterniflora* in its invasive and native ranges. J Plant Ecol. 2021;14: 348–360.

17. Colomer-Ventura F, Martínez-Vilalta J, Zuccarini P, Escolà A, Armengot L, Castells E. Contemporary evolution of an invasive plant is associated with climate but not with herbivory. Funct Ecol. 2015;29: 1475–1485.

18. Alexander JM, Edwards PJ, Poll M, Parks CG, Dietz H. Establishment of parallel altitudinal clines in traits of native and introduced forbs. Ecology. 2009;90: 612–622.

19. Wu Y, Colautti RI. Evidence for continent-wide convergent evolution and stasis throughout 150 y of a biological invasion. Proc Natl Acad Sci U S A. 2022;119: e2107584119.

20. Innes SG, Santangelo JS, Kooyers NJ, Olsen KM, Johnson MTJ. Evolution in response to climate in the native and introduced ranges of a globally distributed plant. Evolution. 2022;76: 1495–1511.

21. Colautti RI, Lau JA. Contemporary evolution during invasion: evidence for differentiation, natural selection, and local adaptation. Mol Ecol. 2015;24: 1999–2017.

22. Bossdorf O, Auge H, Lafuma L, Rogers WE, Siemann E, Prati D. Phenotypic and genetic differentiation between native and introduced plant populations. Oecologia. 2005;144: 1–11.

23. Woods EC, Sultan SE. Post-introduction evolution of a rapid life-history strategy in a newly invasive plant. Ecology. 2022;103: e3803.

24. Yang Y, Liu M, Pan Y, Huang H, Pan X, Sosa A, et al. Rapid evolution of latitudinal clines in growth and defence of an invasive weed. New Phytol. 2021;230: 845–856.

25. Innes SG, Santangelo JS, Kooyers NJ, Olsen KM, Johnson MTJ. Evolution in response to climate in the native and introduced ranges of a globally distributed plant. Evolution. 2022;76: 1495–1511.

26. Westley PAH. What invasive species reveal about the rate and form of contemporary phenotypic change in nature. Am Nat. 2011;177: 496–509.

27. Battlay P, Wilson J, Bieker VC, Lee C, Prapas D, Petersen B, et al. Large haploblocks underlie rapid adaptation in the invasive weed *Ambrosia artemisiifolia*. Nat Commun. 2023;14: 1717.

28. García-Ramos G, Kirkpatrick M. Genetic models of adaptation and gene flow in peripheral populations. Evolution. 1997;51: 21–28.

29. Bolnick DI, Barrett RDH, Oke KB, Rennison DJ, Stuart YE. (Non)Parallel Evolution. Annu Rev Ecol Evol Syst. 2018;49: 303–330.

30. Duputié A, Massol F, Chuine I, Kirkpatrick M, Ronce O. How do genetic correlations affect species range shifts in a changing environment? Ecol Lett. 2012;15: 251–259.

31. Page MJ, McKenzie JE, Bossuyt PM, Boutron I, Hoffmann TC, Mulrow CD, et al. The PRISMA 2020 statement: an updated guideline for reporting systematic reviews. BMJ. 2021;372: n71.

32. Schneider CA, Rasband WS, Eliceiri KW. NIH Image to ImageJ: 25 years of image analysis. Nat Methods. 2012;9: 671–675.

33. Essl F, Dullinger S, Genovesi P, Hulme PE, Jeschke JM, Katsanevakis S, et al. A conceptual framework for range-expanding species that track human-induced environmental change. BioScience. 2019;69: 908–919.

34. Seebens H, Blackburn TM, Dyer EE, Genovesi P, Hulme PE, Jeschke JM, et al. No saturation in the accumulation of alien species worldwide. Nat Commun. 2017;8: 14435.

35. Compagnoni A, Levin S, Childs DZ, Harpole S, Paniw M, Römer G, et al. Herbaceous perennial plants with short generation time have stronger responses to climate anomalies than those with longer generation time. Nat Commun. 2021;12: 1824.

36. Pacifici M, Santini L, Di Marco M, Baisero D, Francucci L, Marasini GG, et al. Generation length for mammals. Nat Conserv. 2013;5: 89–94.

37. Kattge J, Bönisch G, Díaz S, Lavorel S, Prentice IC, Leadley P, et al. TRY plant trait database – enhanced coverage and open access. Glob Chang Biol. 2020;26: 119–188.

38. Staerk J, Conde DA, Ronget V, Lemaitre J, Gaillard J, Colchero F. Performance of generation time approximations for extinction risk assessments. Rhodes J, editor. J Appl Ecol. 2019;56: 1436–1446.

39. R Core Team. R: A Language and Environment for Statistical Computing. R Foundation for Statistical Computing, Vienna, Austria. 2024.

40. Atwater DZ, Ervine C, Barney JN. Climatic niche shifts are common in introduced plants. Nat Ecol Evol. 2018;2: 34–43.

41. Stuart YE, Veen T, Weber JN, Hanson D, Ravinet M, Lohman BK, et al. Contrasting effects of environment and genetics generate a continuum of parallel evolution. Nat Ecol Evol. 2017;1: 158.

42. Carvalho C, Davis R, Connallon T, Gleadow RM, Moore JL, Uesugi A. Multivariate selection mediated by aridity predicts divergence of drought-resistant traits along natural aridity gradients of an invasive weed. New Phytol. 2022;234: 1088–1100.

43. Friedrich JO, Adhikari NK, Beyene J. The ratio of means method as an alternative to mean differences for analyzing continuous outcome variables in meta-analysis: a simulation study. BMC Med Res Methodol. 2008;8: 32.

44. Viechtbauer W. Conducting meta-analyses in R with the metafor package. J Stat Softw. 2010;36: 1–48.

45. Zuur AF, Ieno EN, Walker NJ, Saveliev AA, Smith GM. Mixed Effects Modelling for Nested Data. In: Zuur AF, Ieno EN, Walker N, Saveliev AA, Smith GM, editors. Mixed effects models and extensions in ecology with R. New York, NY: Springer; 2009. pp. 101–142.

46. Knapp G, Hartung J. Improved tests for a random effects meta-regression with a single covariate. Stat Med. 2003;22: 2693–2710.

47. Harrer M, Cuijpers P, Furukawa T, Ebert DD. dmetar: companion R package for the guide "Doing meta-analysis in R." R package version 00. 2019;9000: 2019.

48. Calcagno V, de Mazancourt C. glmulti: an R package for easy automated model selection with (generalized) linear models. J Stat Softw. 2010;34: 1–29.

49. Burnham KP, Anderson DR. Multimodel inference: understanding AIC and BIC in model selection. Sociol Methods Res. 2004;33: 261–304.

50. Nakagawa S, Lagisz M, O'Dea RE, Pottier P, Rutkowska J, Senior AM, et al. orchaRd 2.0: An R package for visualising meta-analyses with orchard plots. Methods Ecol Evol. 2023;14: 2003–2010.

51. Crooks JA. Lag times and exotic species: The ecology and management of biological invasions in slow-motion1. Ecoscience. 2005;12: 316–329.

52. Keller SR, Sowell DR, Neiman M, Wolfe LM, Taylor DR. Adaptation and colonization history affect the evolution of clines in two introduced species. New Phytologist. 2009;183: 678–690.

53. Hodgins KA, Bock DG, Rieseberg LH. Trait evolution in invasive species. Annual Plant Reviews Online. 2018;1: 459–496.

54. Shine R, Brown GP, Phillips BL. An evolutionary process that assembles phenotypes through space rather than through time. Proc Natl Acad Sci U S A. 2011;108: 5708–5711.

55. Polechová J, Barton NH. Limits to adaptation along environmental gradients. Proc Natl Acad Sci U S A. 2015;112: 6401–6406.

56. Štajerová K, Šmilauer P, Brůna J, Pyšek P. Distribution of invasive plants in urban environment is strongly spatially structured. Landsc Ecol. 2017;32: 681–692.

57. Groffman PM, Cavender-Bares J, Bettez ND, Grove JM, Hall SJ, Heffernan JB, et al. Ecological homogenization of urban USA. Front Ecol Environ. 2014;12: 74–81.

58. Rigby LC, Hall MD, Monro K, Uesugi A. Evolution of "invasion syndrome" in invasive goldenrod is not constrained by genetic trade-offs. Evol Appl. 2024;17: e13734.

59. Calsbeek B, Lavergne S, Patel M, Molofsky J. Comparing the genetic architecture and potential response to selection of invasive and native populations of reed canary grass. Evol Appl. 2011;4: 726–735.

60. Franks SJ, Wheeler GS, Goodnight C. Genetic variation and evolution of secondary compounds in native and introduced populations of the invasive plant *Melaleuca quinquenervia*. Evolution. 2012;66: 1398–1412.

61. McGoey BV, Stinchcombe JR. Introduced populations of ragweed show as much evolutionary potential as native populations. Evol Appl. 2021;14: 1436–1449.

62. Sakata Y, Utsumi S, Craig TP, Itami JK, Ikemoto M, Ohgushi T. Environmentally triggered variability in the genetic variance–covariance of herbivory resistance of an exotic plant *Solidago altissima*. Ecol Evol. 2020;10: 3103–3111.

63. Zhang B, Hastings A, Grosholz ED, Zhai L. The comparison of dispersal rate between invasive and native species varied by plant life form and functional traits. Mov Ecol. 2023;11: 73.

64. Phillips BL, Brown GP, Shine R. Evolutionarily accelerated invasions: the rate of dispersal evolves upwards during the range advance of cane toads. J Evol Biol. 2010;23: 2595–2601.

65. Guo Q. Central-marginal population dynamics in species invasions. Front Ecol Evol. 2014;2: 23.

66. Irwin RE, Warren PS, Adler LS. Phenotypic selection on floral traits in an urban landscape. Proc R Soc B Biol Sci. 2018;285: 20181239.

67. Totland Ø. Environment-dependent pollen limitation and selection on floral traits in an alpine species. Ecology. 2001;82: 2233–2244.

68. Geber MA, Griffen LR. Inheritance and natural selection on functional traits. Int J Plant Sci. 2003;164: S21–S42.

69. Johnson MT, Agrawal AA, Maron JL, Salminen J-P. Heritability, covariation and natural selection on 24 traits of common evening primrose (*Oenothera biennis*) from a field experiment. J Evol Biol. 2009;22: 1295–1307.

70. Colautti RI, Barrett SCH. Rapid adaptation to climate facilitates range expansion of an invasive plant. Science. 2013;342: 364–366.

71. Blossey B, Notzold R. Evolution of increased competitive ability in invasive nonindigenous plants: a hypothesis. J Ecol. 1995;83: 887–889.

72. Zangerl AR, Stanley MC, Berenbaum MR. Selection for chemical trait remixing in an invasive weed after reassociation with a coevolved specialist. Proc Natl Acad Sci U S A. 2008;105: 4547–4552.

73. Sakata Y, Yamasaki M, Isagi Y, Ohgushi T. An exotic herbivorous insect drives the evolution of resistance in the exotic perennial herb *Solidago altissima*. Ecology. 2014;95: 2569–2578.

74. Oakeshott JG, Gibson JB, Anderson PR, Knibb WR, Anderson DG, Chambers GK. Alcohol dehydrogenase and glycerol-3-phosphate dehydrogenase clines in *Drosophila melanogaster* on different continents. Evolution. 1982;36: 86–96.

75. Adrion JR, Hahn MW, Cooper BS. Revisiting classic clines in *Drosophila melanogaster* in the age of genomics. Trends Genet. 2015;31: 434–444.

76. Hoffmann AA, Weeks AR. Climatic selection on genes and traits after a 100 year-old invasion: a critical look at the temperate-tropical clines in *Drosophila melanogaster* from eastern Australia. Genetica. 2007;129: 133–147.

77. Kim AS, Kreiner JM, Hernández F, Bock DG, Hodgins KA, Rieseberg LH. Temporal collections to study invasion biology. Mol Ecol. 2023;32: 6729–6742.